*Technical Note*

# The Bias in PPP-B2b Real-Time Clock Offset and the Strategy to Reduce It

Jinhuo Liu [1,2] , Chengpan Tang [1,*], Shanshi Zhou [1], Xiaogong Hu [1], Yufei Yang [3], Jianhua Yang [1,2] and Yuchen Liu [1,2]

1    Shanghai Astronomical Observatory, Chinese Academy of Sciences, Shanghai 200030, China
2    University of Chinese Academy of Sciences, Beijing 100049, China
3    Beijing Satellite Navigation Center, Beijing 100094, China
*    Correspondence: cptang@shao.ac.cn

**Abstract:** Precise point positioning can provide accurate coordinates to users without reference stations, and the high-precision real-time clock offset product is necessary for real-time precise point positioning application. As an integral part of the third generation BeiDou Navigation Satellite System, Precision Point Positioning Service provides dual systems (BDS-3 and GPS) real-time PPP services with centimeter- and decimeter-level accuracy for static and kinematic positioning users around China, respectively. However, there exist inconsistent biases in the clock offset of Precision Point Positioning Service, which will negatively affect the positioning and timing performance of the service. By comparing with the post-processing clock offset, this paper verifies that the broadcast clock offset has smaller and more stable biases in the long term and proposes a regional clock offset estimation strategy using broadcast clock offset for a priori constraint. The results show that the new algorithm can effectively reduce the bias in PPP-B2b clock offset. The new clock offset product could improve convergence speed by 25% and 10% in the horizontal and vertical directions. For positioning accuracy, the improvement is 22% and 17%. The absolute error of timing can also be reduced by 60%.

**Keywords:** BeiDou-3 Navigation Satellite System; real-time clock offset; PPP-B2b service

## 1. Introduction

Precise point positioning (PPP) can provide accurate coordinates to users without reference stations [1] and is widely used in scientific studies, such as oceanography [2] and earthquake early warning [3]. The precision orbit and clock offset for PPP are usually provided by IGS analysis centers. The consistency of GPS, GLONASS, Galileo, and Beidou-2 satellite post-processed clock offset are 2 cm, 5 cm, 5 cm, and 10 cm, respectively [4]. However, the release time is generally delayed by several days. In recent years, with the exploration of GNSS applications, precise products are needed more timely for users of some emerging fields, such as LEO satellite orbit determination [5], unmanned aerial vehicle photogrammetry [6], GNSS meteorology [7], etc.

As an integral part of the third generation BeiDou Navigation Satellite System (BDS-3), Precision Point Positioning Service (PPP-B2b) provides dual system (BDS-3 and GPS) real-time PPP services with centimeter- and decimeter-level accuracy for static and kinematic positioning users, respectively, around China [8,9]. Through the GEO satellite in BDS-3, users of PPP-B2b can obtain PPP-B2b precise clock offset (B2bCO) products with a precision better than 0.3 ns.

Previously, some scholars have evaluated the B2bCO by comparing it with the post-processed product of the analysis center [10,11]. Although there are some numerical differences between these assessments, qualitative conclusions can be drawn: Compared with external products, the B2bCO of each satellite has a different bias, ranging from decimeter to meter, though it is precise enough to support the official positioning accuracy standard. This bias has not been studied in depth before. It is generally believed that the

bias in clock offset may be related to the receiver type [12], algorithm, and the calibration of equipment delay.

The satellite clock offset parameters in the broadcast message of BDS-3 Positioning, Navigation and Timing Service (PNTS) is estimated differently from PPP-B2b. There are two time synchronization methods used in the calculation. The L-band two-way satellite time and frequency transfer (TWSTFT) establishes the satellite ground connection, and the time division multiple access inter-satellite link (ISL) clock offset estimation establishes the inter-satellite connection [13,14]. The former has been successfully applied in the construction of the Beidou-2 regional navigation system [15], but it can only cover 40% arc of the MEO satellite with regional observation [16]. The latter effectively improves the clock offset estimation accuracy of outland BDS-3 satellites without satellite-ground observation. According to the long-term analysis, there is no apparent bias between the clock offset of PNTS and the post-processing.

Based on the characteristics of PNTS clock offset and B2bCO, a regional network clock offset estimation strategy with broadcast clock offset for priori constraint is proposed. According to the strategy, we reconstructed the computing process of PPP-B2b, and obtained then new clock offset product. The results show that the new algorithm effectively reduces the bias in B2bCO. The new clock offset product can improve the convergence speed by about 25% and 10%, and the positioning accuracy after convergence by 22% and 17% in the horizontal and vertical directions, respectively. It can also reduce the absolute error of timing by 60%.

This paper is organized as follows. First of all, in Section 2, the estimation process and the bias of PPP-B2b clock offset is briefly described. Section 3 introduces the new clock offset estimation process and evaluates the new clock offset. In Section 4, the positioning performance and timing performance of the new clock offset and B2bCO are compared and analyzed. The summary and discussion are in the final part.

## 2. The Estimation Process and Bias of PPP-B2b Clock Offset Product

### 2.1. Estimation Process of PPP-B2b Clock Offset Product

The estimation process of the PPP-B2b clock offset product is given in Figure 1. The process is roughly divided into four modules, multi-satellite orbit determination module, real-time OC (Observation minus Calculation) calculation module, clock offset estimation module, and correction calculation module.
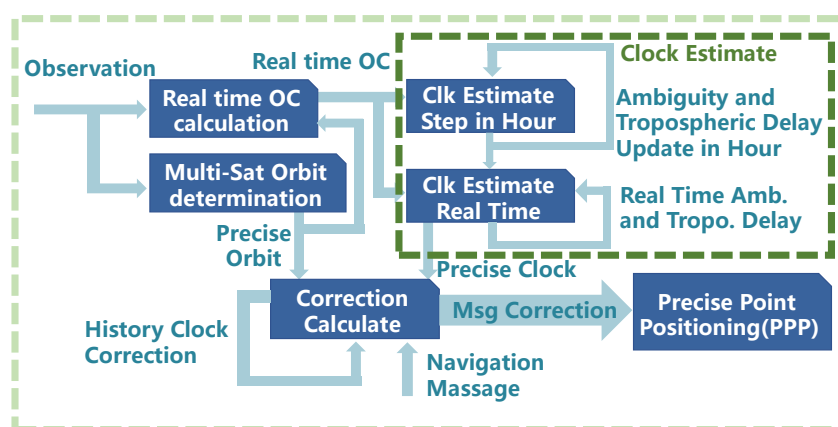


**Figure 1.** Estimation Process of PPP-B2b Clock Offset Product.

In a whole process, the orbit determination was carried out at first using the observation data of the previous three days. The obtained satellite's precise orbit and prediction orbit for several days are saved in memory. Driven by the real-time observation data stream, the real-time OC calculation module uses the orbit in memory to deduct various errors in the observation:

$$\begin{cases} l^s_{PC,r} = PC^s_r - \rho^s_r - T^s_r - (b^s_{IF} + b_{r,IF}) - \epsilon_{PC} \\ l^s_{LC,r} = LC^s_r - \rho^s_r - T^s_r - (\phi^s_{IF} + \phi_{r,IF}) - \lambda N^s_{IF,r} - \epsilon_{LC} \end{cases} \quad (1)$$

The $r$ and $s$ denote the specific receiver and satellite. The $\rho$, $T$, and $N$ represent the geometric distance, tropospheric delay, and ambiguity, respectively. The $l_{PC}$ and $l_{LC}$ is the OC (including satellite and receiver clock offsets) calculated in this module. The real-time OC stream is injected into the clock offset estimation module. The clock offset estimation module includes two sub-modules: hourly estimation and real-time estimation. The hourly estimation sub-module caches the residual stream, filters it in hours, and sends the troposphere and ambiguity information to the real-time estimation module. With the constraint of such corresponding information, the real-time clock offset estimation module, which is driven by the residual stream, estimates the real-time clock offset and saves this unoptimized clock offset into the memory. Finally, using the clock offset, precise orbit, and navigation messages, the correction products are generated after judgment and elimination with historical data in the correction product calculation module.

Among these modules, the multi-satellite orbit determination supported by ISL has been thoroughly studied, and its stability and the accuracy of prediction products can be guaranteed [17–20]. The crux of PPP-B2b is to generate continuous real-time clock offset products with high precision stably. The combination of hourly and real-time filters ensures the stable convergence of the clock offset estimation based on regional observation. Moreover, the estimation process of the PPP-B2b clock offset product is distributed in three independent modules: real-time OC calculation, clock offset estimation, and correction calculation. Even if catastrophic failures occur in the clock offset estimation module (the most probable), the upstream module (real-time OC calculation) and the downstream module (correction calculation) will not be involved. The correction products can be constantly predicted in the correction calculation module within 2 min, and the uninterrupted real-time residual stream facilitates the rapid resumption of the clock offset estimation module.

### 2.2. PPP-B2b Clock Correction and Bias of Clock Offset

The GEO satellite of BDS-3 broadcasts four types of PPP-B2b correction products to users at a rate of 500 bps [8]. The clock correction of all satellites in the mask is broadcast to the user through Message Type 4 in a period of 6 seconds. If the clock offset of a specific satellite is invalid, it is assigned the value of $-26.2128$. Through the PPP-B2b clock correction sent by GEO and the broadcast clock offset (BRCO) of the corresponding satellite, users can obtain B2bCO with:

$$C^i_{B2bCO} = C^i_{BRCO} - \frac{C^i_0}{c} \quad (2)$$

$C^i_0$ is the clock correction of PPP-B2b at epoch $i$, while $C^i_{B2bCO}$ and $C^i_{BRCO}$ are the B2bCO and BRCO at this time; $c$ is the speed of light.

From August 2020 (PPP-B2b on service) to July 2021, a total of 320 days of long-term B2bCO were used for evaluation in order to analyze the value and change of the bias. The post-processed clock offset (PPCO), calculated with the same orbit, PCO, DCB, and the observation data of the same type receiver, was set as the benchmark for evaluation to ensure other effects were eliminated. The bias of B2bCO on a certain day can be extracted as:

$$\begin{cases} \Delta C^i_{B2bCO} = C^i_{B2bCO} - C^i_{PPCO} \\ \Delta C_{B2bCO} = \frac{1}{n} \sum_{i=1}^{n} \Delta C^i_{B2bCO} \end{cases} \quad (3)$$

$i$ is the $i_{th}$ valid epoch of the day (B2bCO and PPCO is both valid); $n$ is the total number of valid epochs in this day; $C^i_{B2bCO}$ and $C^i_{PPCO}$ is the B2bCO and PPCO of the corresponding epoch; $\Delta C_{B2bCO}$ is the bias between B2bCO and PPCO. For a satellite, if its clock offset has two or more effective arcs in a day, the longest one is selected for statistics.

In Figure 2, the X-axis is the number of days from 1 August 2020, the blue dot is the bias of all satellites, and the red line is the $3\sigma$ confidence interval counted by day. The bias still existed after other effects were removed, which indicated that the estimation algorithm or receiver characteristic is a significant source of this bias. The bias can be considered in two parts. The biases of all satellites have the same long-term variation trend, which ranges between $\pm 3$ m. After removing the long-term trend, the biases of satellites are not consistent, with the standard deviation (STD) $\sigma_{Bia}$ of 0.315 m (1.05 ns).
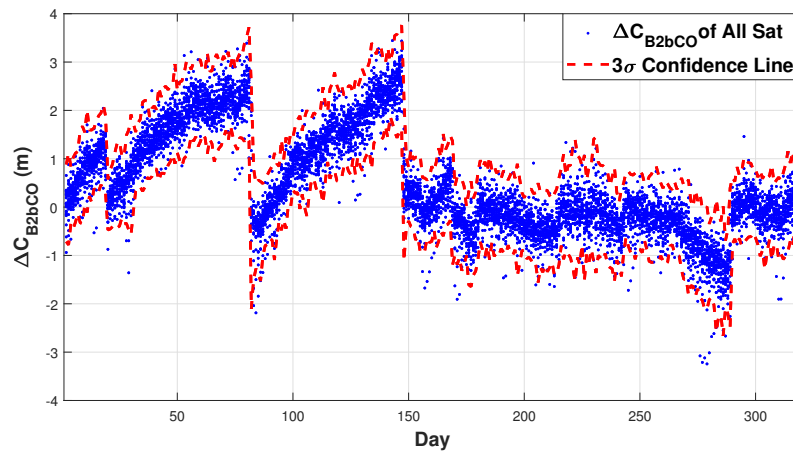


**Figure 2.** The bias of B2bCO changes in the long term.

Although most of the inconsistent biases in B2bCO will be eventually absorbed by ambiguity coefficients in PPP, it will still affect the convergence time and final accuracy of PPP. For static PPP, the impact can be approximately estimated as:

$$\Delta_P = \frac{SigLC}{SigPC} * PDOP * \sigma_{Bia} \tag{4}$$

$SigPC$ and $SigLC$ are the a priori observation noise of pseudo-range and carrier phase, respectively; $PDOP$ is the average position dilution of precision; $\Delta_P$ is the positioning error caused by the inconsistent part of the bias, which is generally around 1 cm to 3 cm. For kinematic PPP, these biases will lead to the divergence of the positioning with the entry and exit of satellites. The order of the divergence is centimeters to decimeters.

The users' receiver clock offset will absorb the consistent part of the bias. It can be inferred from the above that the timing error of PPP-B2b is around $\pm 10$ ns, although the timing performance of PPP-B2b is not given officially.

## 3. Real-Time Algorithm of B2bCO with BRCO Constraint

BRCO and B2bCO are calculated with two different time synchronization systems. BRCO uses L-band TWSTFT and Ka-band Full-ISL to estimate satellite clock offset, while B2bCO is solved with pseudo-range and carrier phase of navigation signal. We are concerned about whether the BRCO is also biased compared with PPCO to confirm the bias is from B2bCO. The comparison is carried out in the same way between BRCO and PPCO:

$$\begin{cases} \Delta C^i_{BRCO} = C^i_{BRCO} - C^i_{PPCO} \\ \Delta C_{BRCO} = \frac{1}{n} \sum_{i=1}^{n} \Delta C^i_{BRCO} \end{cases} \tag{5}$$

$i$ is the $i_{th}$ valid epoch of the day; $C^i_{BRCO}$ and $C^i_{PPCO}$ is the BRCO and PPCO of the corresponding epoch; $\Delta C^i_{BRCO}$ is the difference between BRCO and PPCO on epoch $i$, while $\Delta C_{BRCO}$ is its daily statistic result.

In Figure 3, the X-Axis is the number of days from 1 August 2020, the blue dot is the difference between BRCO and PPCO of all satellites, and the red line is the $3\sigma$ confidence interval counted by day. Compared with B2bCO, there is almost no long-term trend in

the difference between BRCO and PPCO. After removing the long-term trend, its STD is around 0.32 m (1.06 ns), slightly larger than B2bCO. It should be noted that this is a statistical result that aims to illustrate that BRCO has a more negligible bias. Actually, B2bCO is much more precise than BRCO and has much better positioning performance. Because of its smaller bias, the BRCO could be used as a priori constraint for the estimation filter of B2bCO and using more appropriate constraints on satellite clock coefficient, so as to reduce the bias in B2bCO.
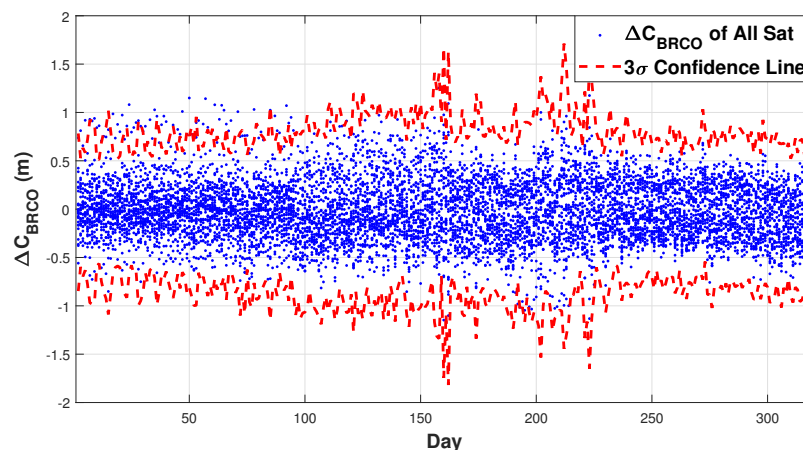


**Figure 3.** The difference between BRCO and PPCO.

### 3.1. The Design of Estimation Process

We reconstructed the process of PPP-B2b as shown in Figure 4. The correction calculation module is divided into long-term and short-term correction calculation modules according to the update period of the output message. Message Type 1 to 3 (mask, orbit correction, and DCB) is calculated in the long-term correction calculation module, while Message Type 4 (clock correction) is calculated in the short-term module. The update period is 48 s and 6 s, respectively. The short-term correction calculation module is combined with the clock offset estimation module so that the historical information and statistical results can be used more flexibly and effectively. Since the stability of the estimation can be guaranteed after the prior information is used more appropriately, the hourly clock offset estimation module is removed to eliminate the hourly jump in B2bCO (around 1 cm to 3 cm) caused by it. Clock correction is now directly generated in the clock offset estimation module.


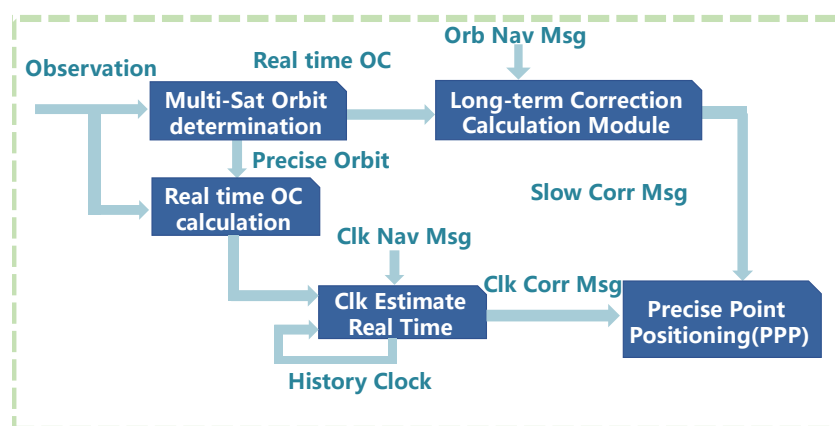
**Figure 4.** Reconstructed PPP-B2b clock offset estimation process.

In the clock offset estimation module, we use two methods to constrain the clock offset coefficients of satellites. When the clock offset sequence is less than 30 min, the BRCO

is used to constrain the coefficients. When the clock offset sequence is longer than 30 min, the historical clock offset sequence is used to predict the clock offset on the current epoch and constrain the coefficients. Different priori noise is needed in different constraint methods.

### 3.2. Priori Noise of BRCO Constraint Method

The BDS-3 navigation broadcast is updated hourly. In order to restrict the clock coefficient appropriately, the RMS of $\Delta C^i_{BRCO}$ (in Formula (5)) is counted according to the time to TOC (Time of Clock). As illustrated in Figure 5, the X-axis is the time to TOC, while the Y-axis is the RMS of $\Delta C^i_{BRCO}$. The dots, which increase linearly, are the RMS of $\Delta C^i_{BRCO}$ counted in minutes between BRCO and PPCO of all satellites. The solid line is the fitting result, and its intercept ($P_0$) and slope ($P_1$) are shown in Table 1.
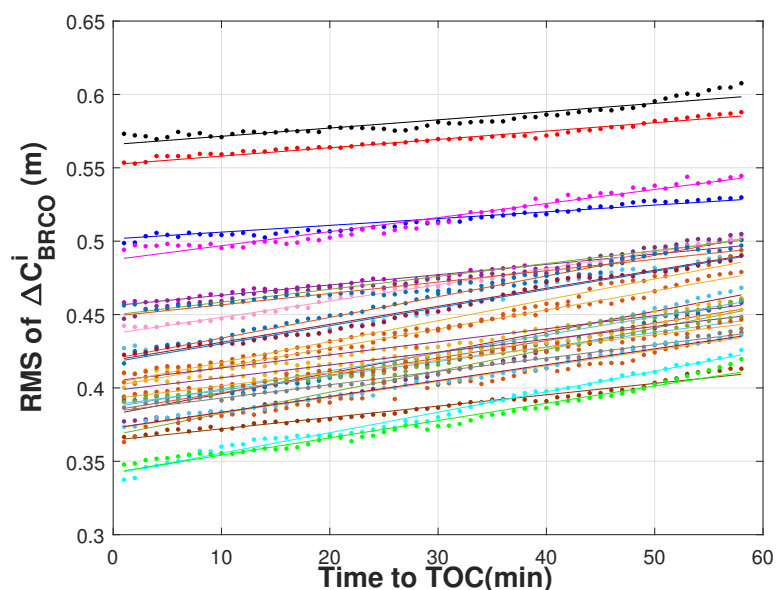


**Figure 5.** The BRCO errors increase with time.

**Table 1.** The fitting result of the BRCO error.

| PRN | $P_1$ | $P_0$ | PRN | $P_1$ | $P_0$ |
|-----|-------|-------|-----|-------|-------|
| C19 | 0.0012 | 0.387 | C34 | 0.0011 | 0.437 |
| C20 | 0.0009 | 0.384 | C35 | 0.0014 | 0.403 |
| C21 | 0.0011 | 0.372 | C36 | 0.0009 | 0.450 |
| C22 | 0.0005 | 0.502 | C37 | 0.0011 | 0.373 |
| C23 | 0.0012 | 0.419 | C38 | 0.0006 | 0.552 |
| C24 | 0.0014 | 0.420 | C39 | 0.0007 | 0.456 |
| C25 | 0.0014 | 0.342 | C40 | 0.0008 | 0.364 |
| C26 | 0.0013 | 0.401 | C41 | 0.0008 | 0.449 |
| C27 | 0.0015 | 0.368 | C42 | 0.0010 | 0.487 |
| C28 | 0.0014 | 0.382 | C43 | 0.0010 | 0.388 |
| C29 | 0.0012 | 0.385 | C44 | 0.0012 | 0.418 |
| C30 | 0.0009 | 0.405 | C45 | 0.0009 | 0.393 |
| C32 | 0.0009 | 0.398 | C46 | 0.0012 | 0.342 |
| C33 | 0.0006 | 0.566 | Average | 0.0010 | 0.416 |

According to the fitting results, the average value of $P_1$ is 0.001. It can be inferred that the error of BRCO increases around 6cm within one hour, which is only about 13% of the

average value of the initial error ($P_0$). We take the $3\sigma$ upper limit of $P_0$ and $P_1$ to estimate the BRCO error:

$$\delta_{\text{BRCO}} = 0.583 + 0.0019dt; \tag{6}$$

$dt$ is the time to TOC. $\delta_{\text{BRCO}}$ is the estimated error of BRCO at this time, which can be used as a priori noise of clock coefficients in the filter.

### 3.3. Priori Noise of Predict Clock Offset Constraint Method

When the clock offset sequence of a satellite is longer than 30 min, the current clock offset value can be predicted with historical information, and the predicted clock offset can be used as a priori constraint of the filter. We assume that the error of the clock offset is composed of the clock speed error and frequency white noise because this prediction is usually shorter than a few minutes. By comparing with the previous epoch, we can obtain the clock speed value $a_1(i)$ of the current epoch and store it. The clock offset in the new epoch can be predicted as:

$$\widetilde{T}_{n+1} = T_n + \frac{dt}{m} \sum_{i=n-m+1}^{n} a_1(i) \tag{7}$$

$n$ is the current epoch; $m$ is the number of epochs used in the prediction; $dt$ is the time interval between epochs; $T_n$ is the clock offset of current epoch, and $\widetilde{T}_{n+1}$ is the predicted clock offset of epoch $n+1$. Considering that the prediction error will be affected by clock drift and white noise, the relations of the errors are:

$$\begin{cases} \sigma_0 = \sqrt{\sigma_{a_2}^2 + \sigma_\varepsilon^2} = std(a_1(n-m+1:n)) \\ \sigma_{\widetilde{T}_{n+1},a_2} = \sqrt{\frac{3(m+1)}{m-1}}\sigma_{a_2} \\ \sigma_{\widetilde{T}_{n+1},\varepsilon} = \sigma_\varepsilon \\ \sigma_{\widetilde{T}_{n+1}} = \sqrt{\sigma_{\widetilde{T}_{n+1},a_2}^2 + \sigma_{\widetilde{T}_{n+1},\varepsilon}^2} \end{cases} \tag{8}$$

$\sigma_0$ is the STD of the clock speed of historical epochs, which is obtained by the saved sequence of $a_1$, while the $\sigma_{\widetilde{T}_{n+1}}$ is the prediction error of $\widetilde{T}_{n+1}$. The errors caused by clock drift and white noise are represented by subscripts $a_2$ and $\varepsilon$, respectively. The error caused by these two parts cannot be accurately estimated, but the following relationship can be obtained:

$$\sigma_0 < \sigma_{\widetilde{T}_{n+1}} < \sqrt{\frac{3(m+1)}{m-1}}\sigma_0 \tag{9}$$

Considering that the prediction is a positive feedback process, that is, too tight constraints will cause the clock offset sequence to be too linear, which leads to tighter constraints. In order to avoid triggering this process, the constraint needs to be loose enough (greater than three times of $\sqrt{\frac{3(m+1)}{m-1}}\sigma_0$), while it should also effectively constrain the clock coefficient. We set the constraint as $8\sigma_0$ after a trail.

### 3.4. Others Coefficients and Strategies of Filter

Except for clock offset, other coefficients of the filter are shown in Table 2. Consistent with the clock coefficients, all types of prior noise and process noise followed the three-sigma rule, such as the observation noise of pseudo-range and carrier phase. Since only observations within China are used, in order to improve the western coverage capability as much as possible, we set the conditions to start estimation as loose as possible. When a satellite is observed by the three receivers above the elevation of $3°$, its clock offset starts to be estimated. The clock offset starts to be output after the estimated time is up to 30 min. We name the clock offset product as Broadcast Constraint Filtering Clock Offset (BCFCO).

**Table 2.** Others coefficients and strategies of the filter.

| Type | Strategy/Coefficient |
|---|---|
| Observation | 9 receivers in China |
| Date | 22 March to 5 April 2022 |
| System | BDS-3 |
| Frequency Combine | B1I/B3I PC + LC |
| Elevation Limit | >3° |
| Interval | 30 s |
| Orbit Product | PPP-B2b Orbit Product |
| Observation Noise | PC: 1 m; LC: 0.01 m |
| Meteorological Model | GPT2.1W + SAAS + VMF1 |
| Trop. Esti. Model | Random Walk,Process Noise 1 cm/h |
| Rcv. Clock Esti. Model | WN, Priori Noise 2 m |
| Amb. Priori Noise | 1.5 m |
| Esti. Method | Kalman Filter |

Trop.: Troposphere; Esti.: Estimation; Sat.: Satellite; Rcv.: Receiver; WN: White Noise; Amb.: Ambiguity.

### 3.5. Analysis of BCFCO

With the PPCO as the standard, the bias and precision of BCFCO are discussed in this section. Compared with B2bCO, the accuracy improvement of BCFCO can be verified and analyzed.

$$\begin{cases} \Delta C^i_{BCFCO} = C^i_{BCFCO} - C^i_{PPCO} \\ \Delta C_{BCFCO} = \frac{1}{n}\sum_{i=1}^{n}\Delta C^i_{BCFCO} \end{cases} \tag{10}$$

The comparison between the bias of BCFCO and B2bCO is given in Figure 6. The X-axis is the number of hours from 00:00 on 22 March 2022; the blue dot is the bias of clock offset, and the red line is the $3\sigma$ confidence interval. The mean value of the bias of BCFCO is stable around 0, while the bias of B2bCO changes around $-0.7$ m. After removing the trend, the average STD of BCFCO is 0.231 m, while the average STD of B2bCO is 0.417 m. It can be confirmed that BCFCO is more accurate than B2bCO.
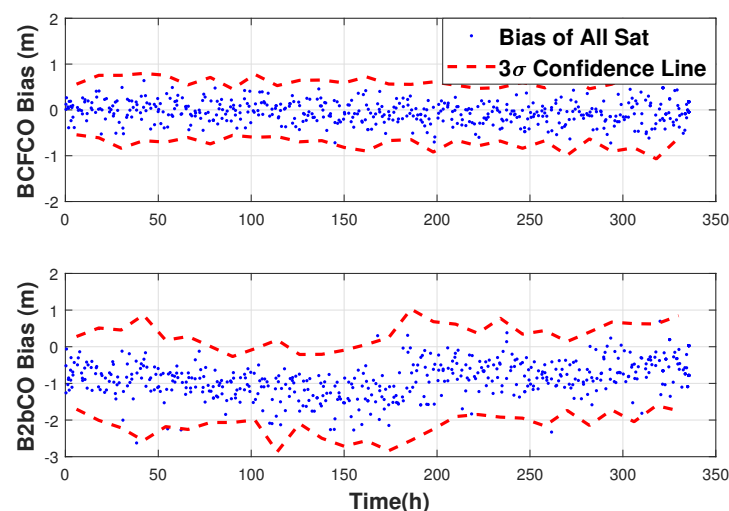


**Figure 6.** The bias of BCFCO and B2bCO.

The precision of BCFCO and B2bCO can be reflected by STD of $\Delta C^i_{BCFCO}$ and $\Delta C^i_{B2bCO}$ after the bias is eliminated. According to the results given in Table 3, the precision of the two kinds of clock offset is basically the same, which illustrates that the new clock offset estimation module can still work stably with appropriate constraints, even if the hourly clock estimation and post-processing module are removed.

**Table 3.** The precision (STD) of clock offset.

| PRN | BCFCO (m) | B2bCO (m) | PRN | BCFCO (m) | B2bCO (m) |
|-----|-----------|-----------|------|-----------|-----------|
| 19 | 0.026 | 0.027 | 34 | 0.016 | 0.014 |
| 20 | 0.034 | 0.033 | 35 | 0.017 | 0.015 |
| 21 | 0.019 | 0.018 | 36 | 0.019 | 0.023 |
| 22 | 0.013 | 0.014 | 37 | 0.022 | 0.022 |
| 23 | 0.015 | 0.017 | 38 | 0.017 | 0.017 |
| 24 | 0.034 | 0.034 | 39 | 0.017 | 0.021 |
| 25 | 0.015 | 0.016 | 40 | 0.017 | 0.017 |
| 26 | 0.037 | 0.038 | 41 | 0.014 | 0.014 |
| 27 | 0.014 | 0.019 | 42 | 0.016 | 0.013 |
| 28 | 0.016 | 0.013 | 43 | 0.017 | 0.017 |
| 29 | 0.017 | 0.015 | 44 | 0.016 | 0.015 |
| 30 | 0.014 | 0.017 | 45 | 0.025 | 0.023 |
| 32 | 0.014 | 0.015 | 46 | 0.017 | 0.017 |
| 33 | 0.015 | 0.017 | mean | 0.020 | 0.021 |

## 4. Timing and Positioning Performance

In PPP, the error on clock offset will have different effects on the positioning results under the influence of various factors. In order to verify the positioning performance of BCFCO products, BCFCO and B2bCO products are compared to discuss the positioning convergence, positioning accuracy, and timing performance of the two products. The observation data of 16 receivers in China were used in the assessment from 22 March to 4 April 2022.

### 4.1. Convergence Performance of Kinematic Positioning

In order to obtain more samples to evaluate the convergence performance, the observation from 1:00 to 23:00 (BDT) each day is divided into 11 segments (2 h for each segment) for kinematic positioning, and the positioning accuracy (RMS) is counted according to the convergence time. In Figure 7, compared with B2bCO, better convergence performance could be achieved using BCFCO products. In the horizontal direction, the 15 min positioning error decreased from 0.38 m to 0.29 m, and the 30-min positioning error decreased from 0.30 m to 0.23 m; In the vertical direction, the 15-min positioning error decreased from 0.40 m to 0.36 m, and the 30-min positioning error decreased from 0.29 m to 0.25 m. The convergence performance in the horizontal direction is improved more significantly than in the vertical direction, which are 25% and 12%, respectively.
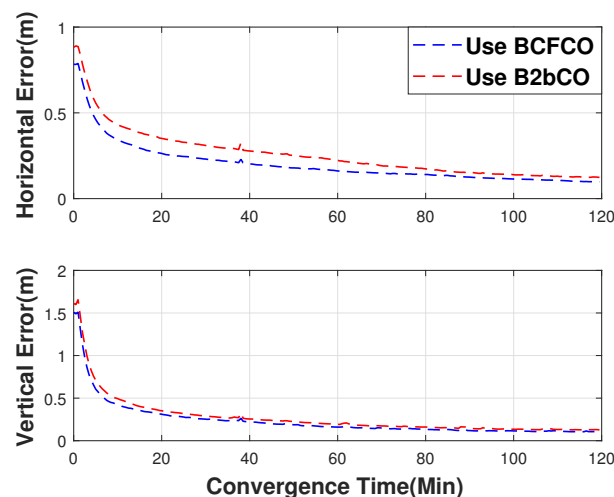


**Figure 7.** Convergence performance of BCFCO and B2bCO.

### 4.2. Accuracy of Kinematic Positioning

Observation data from 1:00 to 23:00 (BDT) is used in BDS-3 single system kinematic positioning, and 95% positioning error is counted from 3:00 to 23:00 each day. Considering that PPP-B2b is a region enhancement system, the positioning performance of receivers is discussed according to their region: Northeast, Northwest, and South of China. In addition, different types of receivers are deployed in some locations to compare the positioning improvement of different types of receivers. The statistical results are shown in Table 4.

**Table 4.** The 95% kinematic positioning accuracy after convergence.

| RcvID | Horizontal Position Error | | | Vertical Position Error | | |
|---|---|---|---|---|---|---|
| | BCFCO | B2bCO | Enhance | BCFCO | B2bCO | Enhance |
| NE1A | 0.084 | 0.104 | 19% | 0.137 | 0.160 | 15% |
| NE2A | 0.061 | 0.086 | 29% | 0.105 | 0.116 | 9% |
| NE3A | 0.066 | 0.102 | 35% | 0.122 | 0.141 | 14% |
| $AVE_{NEA}$ | 0.070 | 0.097 | 28% | 0.121 | 0.139 | 13% |
| NW1A | 0.179 | 0.232 | 23% | 0.307 | 0.334 | 8% |
| NW2A | 0.101 | 0.135 | 25% | 0.164 | 0.260 | 37% |
| NW3A | 0.078 | 0.107 | 27% | 0.112 | 0.144 | 22% |
| $AVE_{NWA}$ | 0.119 | 0.158 | 24% | 0.194 | 0.246 | 21% |
| SC1A | 0.067 | 0.145 | 54% | 0.184 | 0.256 | 28% |
| SC2A | 0.045 | 0.074 | 39% | 0.150 | 0.206 | 27% |
| SC3A | 0.060 | 0.078 | 23% | 0.118 | 0.159 | 26% |
| $AVE_{SCA}$ | 0.057 | 0.099 | 42% | 0.151 | 0.207 | 27% |
| NE1B | 0.151 | 0.175 | 13% | 0.162 | 0.205 | 21% |
| NE2B | 0.084 | 0.101 | 17% | 0.129 | 0.169 | 24% |
| $AVE_{NEB}$ | 0.104 | 0.137 | 24% | 0.156 | 0.206 | 24% |
| NW1B | 0.159 | 0.158 | −1% | 0.342 | 0.329 | −4% |
| NW2B | 0.095 | 0.104 | 9% | 0.153 | 0.163 | 6% |
| NW3B | 0.179 | 0.213 | 16% | 0.244 | 0.274 | 11% |
| $AVE_{NWB}$ | 0.144 | 0.158 | 9% | 0.246 | 0.255 | 4% |
| SC1B | 0.124 | 0.187 | 34% | 0.219 | 0.277 | 21% |
| SC2B | 0.109 | 0.115 | 5% | 0.173 | 0.190 | 9% |
| $AVE_{SCB}$ | 0.126 | 0.153 | 18% | 0.213 | 0.241 | 12% |

The first two digits of the RcvID represent the region (NE is the northeast, NW is the northwest, and the SC is the South). The third digit represents the distance between the receiver and the core region of China (1 represents the receiver in the region farthest away from the core region). The receivers with the same first three letters have the same position. The fourth letter represents the type of receiver ('A' represents the receiver of the same type as the estimation receiver, and 'B' is another type).

In general, the receivers in the northeast can obtain the best positioning accuracy, followed by the south, and the worst in the northwest, which is related to the moving direction of BDS-3 satellites. Most MEO satellites enter China from the West, while IGSO satellites and few MEO satellites will enter from the south. It usually takes dozens of minutes for a satellite from reaching observation conditions to providing services, which results in a greater PDOP in the entry border area. Furthermore, the closer the receiver is to the core area of China, the more obvious the improvement on positioning accuracy is with BCFCO products, except the SC1 location. In all regions, compared with B-type receivers, the A-type receivers can obtain better positioning performance and greater performance improvement using BCFCO, which may be due to the code bias. The average

improvement on the positioning accuracy of BCFCO is 22% and 17% in horizontal and vertical directions, respectively.

*4.3. Timing Performance*

With two calibrated timing receivers TM1A and TM1B, the timing performance of BCFCO and B2bCO can be evaluated by the static PPP. Observation data from 1:00 to 23:00 (BDT) is used and the error of clock offset and clock rate is counted from 3:00 to 23:00 in each day.

The timing performance of two receivers using different products is given in Table 5. Using BCFCO product, the clock offset error of receivers is about 0.9 ns (0.25 m), while it is 2.3 ns (0.69 m) and 3.7 ns (1.17 m) using B2bCO product, which is consistent with the bias of clock offset mentioned in Section 3.5. The clock rate error of the two products is basically the same, about 0.012 ns (0.004 m) per 30 s (step of PPP). This error is generally consistent with receiver observation noise of the carrier phase that determines the upper limit of the clock offset precision. The accurate clock rate of receivers can be obtained with both two products.

**Table 5.** Statistical results of timing performance of TM1A and TM1B.

| STAID | Clock Offset Error (ns) | | Clock Rate Error (ns/30 s) | |
|---|---|---|---|---|
| | **BCFCO** | **B2bCO** | **BCFCO** | **B2bCO** |
| TM1A | 0.76 | 2.27 | 0.010 | 0.012 |
| TM1B | 0.88 | 3.74 | 0.013 | 0.013 |

## 5. Summary and Conclusions

This paper focuses on the bias that exists in PPP-B2b precision clock offset products (B2bCO). Firstly, the estimation process of PPP-B2b clock offset product is introduced, and then bias in B2bCO is analyzed with long-term historical data and post-processing clock offset (PPCO). According to the analysis, we propose a regional clock offset estimation strategy using broadcast clock offset for a priori constraint and get the new clock offset product (BCFCO). By comparing with the B2bCO, the performance improvement of BCFCO on the accuracy of clock offset, dynamic positioning, and timing is discussed.

The bias in B2bCO can be considered in two parts. The biases of all satellites have the same long-term variation trend, which ranges between ±3 m. After removing the long-term trend, the biases of satellites are not consistent, with the STD of 0.315 m (1.05 ns). In PPP, the consistent part of the bias will be absorbed into the receiver clock offset, while the inconsistent part will affect the convergence time and positioning accuracy. BCFCO has better accuracy and similar precision than B2bCO. The consistent part of BCFCO is almost eliminated, and the inconsistent part was reduced by 45%. The precision of the two clock offset products is both about 0.02 m.

The BCFCO and B2bCO are contrasted in terms of speed of convergence, positioning accuracy, and timing. Using BCFCO, the convergence speed increases by about 25% and 10% in horizontal and vertical directions, respectively. For the positioning accuracy, the average improvement is 22% and 17%. The closer it is to the core service area of China, the more obvious the improvement is. The improvement on the receivers of the same type is more obvious than that of receivers of another type. For timing, the error of the receiver clock offset can be reduced by 60% with the BCFCO product, while the error of clock rate is basically the same.

**Author Contributions:** Conceptualization, C.T., J.Y. and Y.L.; Data curation, Y.Y.; Formal analysis, J.L.; Resources, Y.Y.; Software, J.L.; Supervision, S.Z. and X.H.; Writing—original draft, J.L.; Writing— review & editing, C.T. and S.Z. All authors have read and agreed to the published version of the manuscript.

**Data Availability Statement:** Not applicable

**Conflicts of Interest:** The authors declare no conflict of interest.

## References

1. Kouba, J.; Héroux, P. Precise Point Positioning Using IGS Orbit and Clock Products. *GPS Solut.* **2001**, *5*, 12–28. [CrossRef]
2. Liu, R.; Guo, B.; Zhang, A.; Yimwadsana, B. Research on GPS precise point positioning algorithm with a Sea Surface Height Constraint. *Ocean Eng.* **2020**, *197*, 106826. [CrossRef]
3. Geng, J.; Bock, Y.; Melgar, D.; Crowell, B.W.; Haase, J.S. A new seismogeodetic approach applied to GPS and accelerometer observations of the 2012 Brawley seismic swarm: Implications for earthquake early warning. *Geochem. Geophys. Geosyst.* **2013**, *14*, 2124–2142. [CrossRef]
4. Steigenberger, P.; Montenbruck, O. Consistency of MGEX Orbit and Clock Products. *Engineering* **2020**, *6*, 898–903. [CrossRef]
5. Bock, H.; Hugentobler, U.; Beutler, G. Kinematic and Dynamic Determination of Trajectories for Low Earth Satellites Using GPS. In *First CHAMP Mission Results for Gravity, Magnetic and Atmospheric Studies*; Reigber, C., Lühr, H., Schwintzer, P., Eds.; Springer: Berlin/Heidelberg, Germany, 2003; pp. 65–69._10. [CrossRef]
6. Grayson, B.; Penna, N.T.; Mills, J.P.; Grant, D.S. GPS precise point positioning for UAV photogrammetry. *Photogramm. Rec.* **2018**, *33*, 427–447. [CrossRef]
7. Dousa, J.; Vaclavovic, P. Real-time zenith tropospheric delays in support of numerical weather prediction applications. *Adv. Space Res.* **2014**, *53*, 1347–1358. [CrossRef]
8. China Satellite Navigation Office. BeiDou Navigation Satellite System Signal In Space Interface Control Document, Precise Point Positioning Service Signal PPP-B2b (Version 1.0). 2022. Available online: http://en.beidou.gov.cn/SYSTEMS/ICD/ (accessed on 12 August 2022).
9. China Satellite Navigation Office. The Application Service Architecture of BeiDou Navigation Satellite System. 2022. Available online: http://en.beidou.gov.cn/SYSTEMS/ICD/ (accessed on 12 August 2022).
10. Xu, Y.; Yang, Y.; Li, J. Performance evaluation of BDS-3 PPP-B2b precise point positioning service. *GPS Solut.* **2021**, *25*, 1–14. [CrossRef]
11. Ren, Z.; Gong, H.; Peng, J.; Tang, C.; Huang, X.; Sun, G. Performance assessment of real-time precise point positioning using BDS PPP-B2b service signal. *Adv. Space Res.* **2021**, *68*, 3242–3254. [CrossRef]
12. Hauschild, A.; Steigenberger, P.; Montenbruck, O. Inter-Receiver GNSS Pseudorange Biases and Their Effect on Clock and DCB Estimation. In Proceedings of the 32nd International Technical Meeting of the Satellite Division of The Institute of Navigation, Miami, FL, USA, 16–20 September 2019; pp. 3675–3685. [CrossRef]
13. Pan, J.; Hu, X.; Zhou, S.; Tang, C.; Guo, R.; Zhu, L.; Tang, G.; Hu, G. Time synchronization of new-generation BDS satellites using inter-satellite link measurements. *Adv. Space Res.* **2018**, *61*, 145–153. [CrossRef]
14. Pan, J.; Hu, X.; Zhou, S.; Tang, C.; Wang, D.; Yang, Y.; Dong, W. Full-ISL clock offset estimation and prediction algorithm for BDS3. *GPS Solut.* **2021**, *25*, 140. [CrossRef]
15. Zhou, S.S.; Hu, X.G.; Liu, L.; Guo, R.; Zhu, L.F.; Chang, Z.Q.; Tang, C.P.; Gong, X.Q.; Li, R.; Yu, Y. Applications of two-way satellite time and frequency transfer in the BeiDou navigation satellite system. *Sci. China Phys. Mech. Astron.* **2016**, *59*, 109511. [CrossRef]
16. Zhou, S.; Hu, X.; Zhou, J.; Chen, J.; Gong, X.; Tang, C.; Wu, B.; Liu, L.; Guo, R.; He, F.; et al. Accuracy analyses of precise orbit determination and timing for COMPASS/Beidou-2 4GEO/5IGSO/4MEO constellation. In Proceedings of the China Satellite Navigation Conference (CSNC), Wuhan, China, 15–17 May 2013; Volume 245, pp. 89–102._8. [CrossRef]
17. Yang, Y.; Yang, Y.; Hu, X.; Chen, J.; Guo, R.; Tang, C.; Zhou, S.; Liqian, Z.; Xu, J. Inter-Satellite Link Enhanced Orbit Determination for BeiDou-3. *J. Navig.* **2019**, *73*, 1–16. [CrossRef]
18. Zhou, S.; Hu, X.; Wu, B.; Liu, L.; Qu, W.; Guo, R.; He, F.; Cao, Y.; Wu, X.; Zhu, L.; et al. Orbit determination and time synchronization for a GEO/IGSO satellite navigation constellation with regional tracking network. *Sci. China Phys. Mech. Astron.* **2011**, *54*, 1089–1097. [CrossRef]
19. Xie, X.; Geng, T.; Zhao, Q.; Cai, H.; Zhang, F.; Wang, X.; Meng, Y. Precise orbit determination for BDS-3 satellites using satellite-ground and inter-satellite link observations. *GPS Solut.* **2019**, *23*, 1–12. [CrossRef]
20. Liqian, Z.; Hu, X.; Tang, C.; Zhou, S.; Cao, Y.; Wang, Q.; Su, R. Inter-satellite link augmented BeiDou-3 orbit determination for Precise Point Positioning. *Chin. J. Aeronaut.* **2021**, *35*, 332–343. [CrossRef]